Pak. J. Biochem. Mol. Biol. 2011; 44(4): 141-147

Conformational analysis and geometry optimization of Febuxostat as a xanthine oxidase inhibitor

Khalida Bano[1], Uzma Asif[1], Asif Khan Sherwani[1], M. Harris Shoaib[2] and Naheed Akhtar[1]*
[1]Biophysics Research Unit, Department of Biochemistry, University of Karachi, Karachi, Pakistan
[2]Department of Pharmaceutics, Faculty of Pharmacy, University of Karachi, Karachi, Pakistan

ABSTRACT: Uric acid is the end product of purine metabolism, elevation of it can cause Gout. Febuxostat is a novel non-purine selective inhibitor of xanthine oxidase being developed for the management of hyperuricaemia in patients with gout. Conformational analysis and geometry optimization of Febuxostat was performed according to the Hartree-Fock (HF) calculation method by Argus Lab 4.0.1 software. The minimum potential energy was found to be -80598.933 kcal/mol. It is the most feasible position for the drug to interact with the receptor.

Keywords: Febuxostat, xanthine oxidase, Hartree-Fock, geometry optimization, Argus Lab-4.0.1.
Received: October 15, 2011 **Accepted:** November 22, 2011
***Author for Correspondence:** khalidabano@hotmail.com

INTRODUCTION

Gout is an increasingly common rheumatic disease. Global studies have found an increase in mean serum urate in both genders during the past four decades[1-3]. Gout is an inflammatory arthritis characterized by self-limiting but excruciatingly painful acute attacks. These are a consequence of monosodium urate (MSU) crystal deposition within articular or periarticular tissue. After years of acute intermittent gout, chronic tophaceous gout can develop. Tophi, nodular masses of uric acid (UA) crystals, can form anywhere but most commonly affect finger tips or hands. Recent advances in understanding of intracellular events have occurred along with new treatment development[4]. Crystal deposition is asymptomatic, but it is revealed by bouts of joint inflammation gouty attacks[5-7]. A major aim in gout management is the long-term reduction of serum uric acid concentrations below saturation levels, as these results in crystal dissolution and eventual disappearance. According to guidelines[6] from the European League Against Arthritis, the treatment goal for chronic gout is to reduce and maintain serum uric acid levels below 6 mg per dl[5-7].

Uric acid is an end-product of purine metabolism in humans and other mammalian species, and is the result of the step-wise actions of the enzyme xanthine oxidase/xanthine dehydrogenase, which converts the purine breakdown product hypoxanthine (via xanthine) to uric acid[8, 10]. Inhibition of xanthine oxidase/xanthine dehydrogenase by the purine analog allopurinol results in decreased serum uric acid levels and improved prognosis for gout. However, some individuals may not tolerate allopurinol owing to a potentially lethal hypersensitivity syndrome.[9, 10] Due to these effects, a need for a better option results in formation of FEBUXOSTAT. Febuxostat (also known as TEI-6720, TMX-67 and Uloric™; Takeda Pharmaceuticals, Deerfield, IL) is an orally-administered inhibitor of xanthine oxidase that was approved for the treatment of chronic hyperuricemia and gout in 2008 in Europe and in 2009 in the US. Febuxostat has a number of biochemical and pharmacodynamic differences from allopurinol, suggesting that, in some patients at least, it may represent a better option for serum urate management[10]. Febuxostat is a potent, selective, non purine inhibitor of Xanthine oxidase[11] which selectively inhibits XO independent of the redox state and does not affect other enzymatic pathways in purine/pyrimidine metabolism[4]. Febuxostat 10-120 mg/day rapidly and sustainably reduces serum uric acid by 25-70% in uric acid under-excretors and overproducers[12,13]. This orally administered drug acts by binding into a channel in the molybdenum center of the enzyme, leading to a very stable and long-lived enzyme-inhibitor interaction with both the oxidized and reduced forms of the enzyme and, as a consequence, a strong inhibition of substrate binding[11,14].

The present work describes the computer aided conformational analysis that is based on geometry optimization (active conformation) of drug by ArgusLab software[16]. Argus Lab is the electronic structure program that is based on the quantum mechanics, it predicts the potential energies, molecular structures; geometry optimization of structure, vibration frequencies of coordinates of atoms, bond length, bond angle and reactions pathway[17]. Conformational analysis of molecule is based on molecular mechanics, it is method for the calculation of molecular structures, conformational energies and other molecular properties using

concept from classical mechanics. A molecule is considered as a collection of atoms held together by classical forces. These forces are described by potential energy function of structural features like bond lengths, bond angles and torsion angles etc. The energy (E) of the molecule is calculated as a sum of terms as in equation:

$E = E_{stretching} + E_{bending} + E_{torsion} + E_{Vander\ Waals} + E_{electrostatic} + E_{hydrogen\ bond}$ + cross term

These terms are of importance for the accurate calculation of geometric properties of molecules. The set of energy functions and the corresponding parameters are called a force field[15,16]. Molecular mechanics potential energy functions (MMPEFs) incorporate both `bonded' and `non-bonded' terms. The bonded terms apply to set of sets of two or four atoms that are covalently linked, and they serve to constrain bond lengths and angles near their equilibrium values. The bonded terms also include a torsional potential that models the periodic energy barriers encountered during bond rotation. The non-bonded terms consist of the Lennard-Jones (L J) function (which includes van der Waals attraction and repulsion owing to orbital overlap) and Coulomb's Law. The parameters for the bonded and non-bonded terms of MM-PEFs are derived from Quantum calculations and from thermodynamic, crystallographic and spectroscopic data on a wide range of systems. MM-PEFs have been used predominately to stimulate protein folding and dynamics, are also used to refine X-ray Crystal Structures[16].

MATERIALS AND METHODS

The three dimensional quantitative structure activity relationships (3D-QSAR) describe the biological activity of molecule with pharmacological potential as a function of their structural properties[15,17,18]. Computational advances have generated many tools which are widely used to construct models, minimization and representations of molecular structure[15,16]. All conformational analysis (geometry optimization) study was performed on a window based computer using Argus lab and ACD Lab Chem Sketch softwares. The Febuxostat molecule is utilized to determine 3D structure of molecule. Several computer programs were used to infer the shape of molecule from geometry optimization calculations. The Febuxostat structure is generated by Argus lab, and minimum potential energy is calculated by using geometry convergence function in Argus lab software. In order to determine the allowed conformation the contact distance between the atoms in adjacent residues is examined using criteria for minimum Vander Waal contact distances[15,16].

Surfaces created to visualize ground state properties as well as excited state properties such as orbital, electron densities, electrostatic potential (ESP) spin densities and generated the grid data used to make molecular orbital surfaces and visualized he molecular orbital and making an electro static potential mapped and electron density surface. The minimum potential energy was calculated for drug receptor interaction through the geometry convergence map.

RESULTS

Prospective view and calculated properties of Febuxostat molecule are shown in figure 1. The active conformation and electron density mapped of Febuxostat by ACDLABS-3D viewer software are shown in figures 2 and 3 respectively.

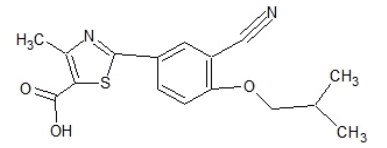

2-[3-cyano-4-(2-methylpropoxy)phenyl]-4-methyl-1,3-thiazole-5-carboxylic acid

Molecular Formula	= $C_{16}H_{16}N_2O_3S$
Formula Weight	= 316.37484
Composition	= C(60.74%) H(5.10%) N(8.85%) O(15.17%) S(10.14%)
Molar Refractivity	= 83.09 ± 0.4 cm^3
Molar Volume	= 240.9 ± 5.0 cm^3
Parachor	= 681.0 ± 6.0 cm^3
Index of Refraction	= 1.605 ± 0.03
Surface Tension	= 63.7 ± 5.0 dyne/cm
Density	= 1.31 ± 0.1 g/cm^3
Dielectric Constant	= Not available
Polarizability	= 32.94 ± 0.5 $10^{-24}cm^3$
Monoisotopic Mass	= 316.088162 Da
Nominal Mass	= 316 Da
Average Mass	= 316.3748 Da

Figure 1: Prospective view and properties of Febuxostat molecule.

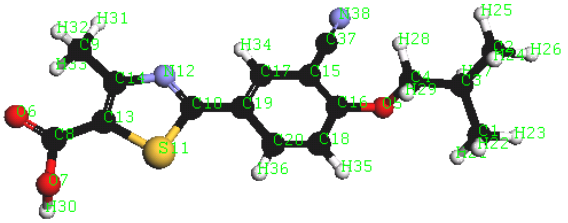

Figure 2: Prospective view of active conformation of Febuxostat.

Figure 4 shows Electrostatic potential of molecular ground state mapped onto the electron density surface for the ground state and in Figure 5,

the complete surface with the colour map is shown. Figure 4 and 5 use a clipping plane showing the cutaway of the same surface revealing the underlying molecular structure.

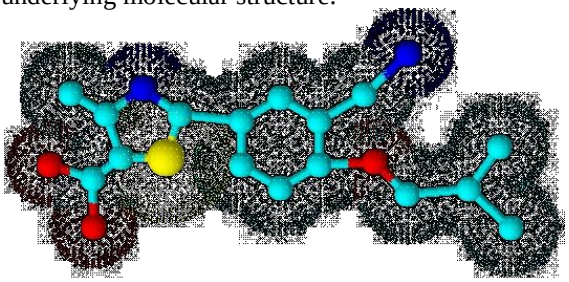

Figure 3: Electron density clouds generated by ACD LABS 3D Viewer.

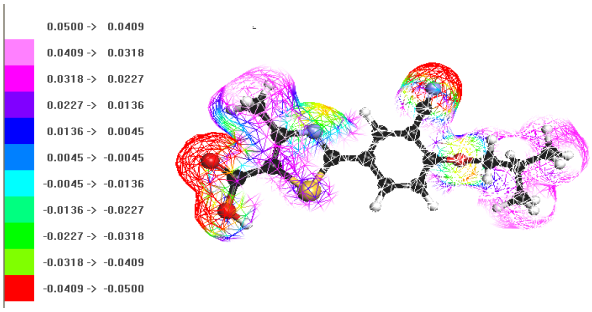

Figure 4: Electrostatic potential (ESP) mapped electron density.

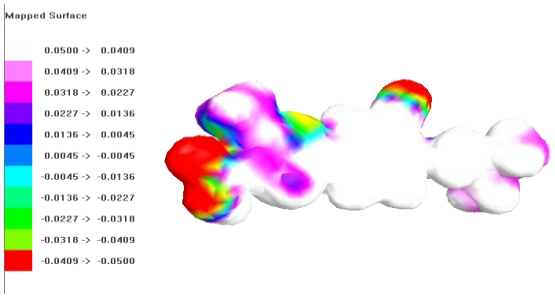

Figure 5: The complete surface with color map of ESP.

The color map shows the ESP energy (in hartrees) for the various colors. The red end of the spectrum shows regions of highest stability for a positive test charge, magenta/ blue show the regions of least stability for a positive test charge. Figure 6 a and 6b show the occupied molecular orbital of molecule calculated with the Zindo method and rendered a mesh the positive and negative phases of the orbital are represented by two colors, the blue regions represent an increase in electron density and the red regions shows a decrease in electron density. This type of surface representations is useful to discuss drug receptor interaction.

Coordination of molecule are given in Table 1 and bond length and bond angles are given in table 2 and 3 respectively, which are calculated after geometry optimization of molecule from ARGUS LAB by using molecular mechanics calculation. Tables 4 shows the dihedral angles and Improper torsion angles of Febuxostat. Table 5 shows calculated energy of Febuxostat molecule. Graph no 1 illustrate the potential energy geometry convergence map of Febuxostat.

Table 1: Co-ordinates of Febuxostat.

Atoms	X	Y	Z
C1	18.745	-12.894	-0.344
C2	20.281	-11.496	1.076
C3	19.321	-11.489	-0.119
C4	18.200	-10.462	0.095
O5	17.405	-10.347	-1.114
O6	9.0322	-4.032	0.596
O7	8.486	-6.210	1.136
C8	9.404	-5.234	0.686
C9	11.678	-3.417	-0.228
C10	12.991	-6.811	-0.158
S11	11.364	-7.332	0.396
N12	13.042	-5.518	-0.352
C13	10.784	-5.635	0.333
C14	11.789	-4.843	-0.072
C15	16.447	-8.156	-1.106
C16	16.327	-9.465	-0.847
C17	15.313	-7.242	-0.858
C18	15.046	-9.997	-0.334
C19	14.142	-7.716	-0.388
C20	14.0154	-9.172	-0.112
H21	18.0754	-12.903	-1.233
H22	18.166	-13.229	0.546
H23	19.570	-13.621	-0.527
H24	21.106	-12.224	0.902
H25	19.743	-11.778	0
H26	20.734	-10.4873	1.211
H27	19.900	-11.1970	-1.027
H28	18.657	-9.471	0.335
H29	17.566	-10.784	0.959
H30	8.023	-6.560	0.280
H31	11.593	-2.365	-0.340
H32	15.446	-6.187	-1.074
H33	14.943	-11.060	-0.139
H34	13.086	-9.583	0.268
N35	18.680	-7.216	-2.060
C36	17.679	-7.639	-1.631

Table 2: Bond length.

No.	Atoms	Bond Length	Alternative Bond Length
1	(C1)-(C3)	1.51	349.79
2	(C2)-(C3)	1.51	349.79
3	(C3)-(C4)	1.51	349.79
4	(C4)-(O5)	1.43	492.98
5	(O5)-(16)	1.40	523.50
6	(O6)-(C8)	1.26	729.47
7	(O7)-(C8)	1.41	520.11
8	(C8)-(C13)	1.46	389.26
9	(C9)-(C14)	1.43	410.81
10	(C10)-(S11)	1.81	287.92
11	(C10)-(N12)	1.30	731.86
12	(C10)-(C19)	1.45	391.67
13	(S11)-(C13)	1.81	287.92
14	(N12)-(C14)	1.43	547.97
15	(C13)-(C14)	1.32	523.76
16	(C15)-(C16)	1.32	523.76
17	(C15)-(C17)	1.45	391.67
18	(C16)-(C18)	1.45	391.67
19	(C17)-(C19)	1.32	523.76
20	(C18)-(C20)	1.32	523.76
21	(C19)-(C20)	1.45	391.67
22	(C15)-(C36)	1.43	410.81
23	(N35)-(C36)	1.16	1013.06
24	(C1)-(H21)	1.11	328.22
25	(C1)-(H22)	1.11	328.22
26	(C1)-(H23)	1.11	328.22
27	(C2)-(H24)	1.11	328.22
28	(C2)-(H25)	1.11	328.22
29	(C2)-(H26)	1.11	328.22
30	(C3)-(H27)	1.11	328.22
31	(C4)-(H28)	1.11	328.22
32	(C4)-(H29)	1.11	328.22
33	(O7)-(H30)	1.03	492.25
34	(C9)-(H31)	1.06	377.87
35	(C17)-(H32)	1.08	354.32
36	(C18)-(H33)	1.08	354.32
37	(C20)-(H34)	1.08	354.32

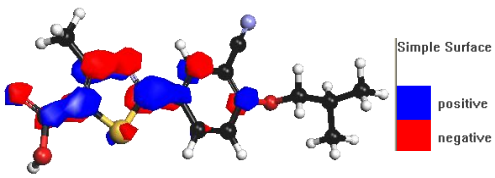

Figure 6a: Visualize the HOMO Orbitals.

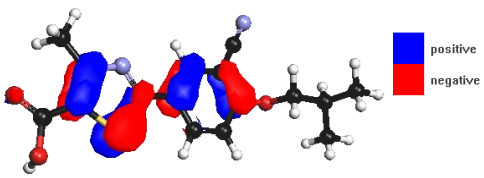

Figure 6b: Visualize the LUMO orbital.

Table 3: Bond angles

No.	Atoms	Bond Angles	Alternate Angles
1	(C1)-(C3)-(C2)	109.47	214.21
2	(C1)-(C3)-(C4)	109.47	214.21
3	(C3)-(C1)-(H21)	109.47	116.98
4	(C3)-(C1)-(H22)	109.47	116.98
5	(C3)-(C1)-(H23)	109.47	116.98
6	(C1)-(C3)-(H27)	109.47	116.98
7	(C2)-(C3)-(C4)	109.47	214.21
8	(C3)-(C2)-(H24)	109.47	116.98
9	(C3)-(C2)-(H25)	109.47	116.98
10	(C3)-(C2)-(H26)	109.47	116.98
11	(C2)-(C3)-(H27)	109.47	116.98
12	(C3)-(C4)-(O5)	109.47	278.25
13	(C4)-(C3)-(H27)	109.47	116.98
14	(C3)-(C4)-(H28)	109.47	116.98
15	(C3)-(C4)-(H29)	109.47	116.98
16	(C4)-(O5)-(C16)	104.51	293.43
17	(O5)-(C4)-(H28)	109.47	156.11
18	(O5)-(C4)-(H29)	109.47	156.11
19	(O5)-(C16)-(C15)	120.00	275.57
20	(O5)-(C16)-(C18)	120.00	238.73
21	(O6)-(C8)-(O7)	120.00	353.33
22	(O6)-(C)8-(C13)	120.00	276.93
23	(O7)-(C8)-(C13)	120.00	237.23
24	(C8)-(O7)-(H30)	104.51	163.31
25	(C8)-(C13)-(S11)	120.00	185.39
26	(C8)-(C13)-(C14)	120.00	215.76
27	(C9)-(C14)-(N12)	120.00	263.30
28	(C9)-(C14)-(C13)	120.00	222.15
29	(C14)-(C9)-(H31)	180.00	58.10
30	(S11)-(C10)-(N12)	120.00	280.75
31	(S11)-(C10)-(C19)	120.00	185.85
32	(C10)-(S11)-(C13)	92.20	201.54
33	(N12)-(C10)-(C19)	120. 00	294.48
34	(C10)-(N12)-(C14)	120.00	227.50
35	(C10)-(C19)-(C17)	120.00	216.48
36	(C10)-(C19)-(C20)	120.00	188.44
37	(S11)-(C13)-(C14)	120.00	207.40
38	(N12)-(C14)-(C13)	120.00	295.98
39	(C16)-(C15)-(C17)	120.00	216.48
40	(C15)-(C16)-(C18)	120.00	216.48
41	(C16)-(C15)-(C36)	120.000	222.15
42	(C15)-(C17)-(C19)	120.00	216.48
43	(C17)-(C15)-(C36)	120.00	192.95
44	(C15)-(C17)-(H32)	120.00	102.92
45	(C16)-(C18)-(C20)	120.00	216.48
46	(C16)-(C18)-(H33)	120.00	102.92
47	(C17)-(C19)-(C20)	120.00	216.48
48	(C19)-(C17)-(H32)	120.00	123.03
49	(C18)-(C20)-(C19)	120.00	216.48
50	(C20)-(C18)-(H33)	120.00	123.03
51	(C18)-(C20)-(H34)	120.00	123.03
52	(C19)-(C20)-(H34)	120.00	102.92
53	(C15)-(C36)-(N35)	180.00	183.11
54	(H21)-(C1)-(H22)	109.47	74.84
55	(H21)-(C1)-(H23)	109.47	74.84
56	(H22)-(C1)-(H23)	109.47	74.84
57	(H24)-(C2)-(H25)	109.47	74.84
58	(H24)-(C2)-(H26)	109.47	74.84
59	(H25)-(C2)-(H26)	109.47	74.84

Table 4: Dihedral angles

No	Atoms	Angles	Alternate angles
1	(H21)-(C1)-(C3)-(C2)	0.23	180.0
2	(H22)-(C1)-(C3)-(C2)	0.23	180.0
3	(H23)-(C1)-(C3)-(C2)	0.23	180.0
4	(C1)-(C3)-(C2)-(H24)	0.23	180.0
5	(C1)-(C3)-(C2)-(H25)	0.23	180.0
6	(C1)-(C3)-(C2)-(H26)	0.23	180.0
7	(H21)-(C1)-(C3)-(C4)	0.23	180.0
8	(H22)-(C1)-(C3)-(C4)	0.23	180.00
9	(H23)-(C1)-(C3)-(C4)	0.23	180.00
10	(C1)-(C3)-(C4)-(O5)	0.23	180.00
11	(C1)-(C3)-(C4)-(H28)	0.23	180.00
12	(C1)-(C3)-(C4)-(H29)	0.23	180.00
13	(H27)-(C3)-(C1)-(H21)	0.23	180.00
14	(H27)-(C3)-(C1)-(H22)	0.23	180.00
15	(H27)-(C3)-(C1)-(H23)	0.23	180.00
16	(H24)-(C2)-(C3)-(C4)	0.23	180.00
17	(H25)-(C2)-(C3)-(C4)	0.23	180.00
18	(H26)-(C2)-(C3)-(C4)	0.23	180.00
19	(C2)-(C3)-(C4)-(O5)	0.23	180.00
20	(C2)-(C3)-(C4)-(H28)	0.23	180.00
21	(C2)-(C3)-(C4)-(H29)	0.23	180.00
22	(H27)-(C3)-(C2)-(H24)	0.23	180. 00
23	(H27)-(C3)-(C2)-(H25)	0.23	180.00
24	(H27)-(C3)-(C2)-(H26)	0.23	180.00
25	(H27)-(C3)-(C4)-(O5)	0.23	180.00
26	(C3)-(C4)-(O5)-(C16)	0.06	180.00
27	(H28)-(C4)-(C3)-(H27)	0.23	180.00
28	(H29)-(C4)-(C3)-(H27)	0.23	180.00
29	(H28)-(C4)-(O5)-(C16)	0.06	180.00
30	(H29)-(C4)-(O5)-(C16)	0.06	180.00
31	(C4)-(O5)-(C16)-(C15)	5.00	90.00
32	(C4)-(O5)-(C16)-(C18)	5.00	90.00
33	(O5)-(C16)-(C15)-(C17)	9.74	180.00
34	(O5)-(C16)-(C15)-(C36)	9.74	180. 00
35	(O5)-(C16)-(C18)-(C20)	2.50	180.00
36	(O5)-(C16)-(C18)-(H33)	2.50	180.00
37	(O6)-(C8)-(O7)-(H30)	5.00	90.00
38	(O6)-(C8)-(C13)-(S11)	2.50	180.00
39	(O6)-(C8)-(C13)-(C14)	2.50	180.00
40	(H30)-(O7)-(C8)-(C13)	5.00	90.00
41	(O7)-(C8)-(C13)-(S11)	2.50	180.00
42	(O7)-(C8)-(C13)-(C14)	2.50	180.00
43	(C8)-(C13)-(S11)-(C10)	3.95	180.00
44	(C8)-(C13)-(C14)-(C9)	9.74	180.00
45	(C8)-(C13)-(C14)-(N12)	9.74	180. 00
46	(C9)-(C14)-(N12)-(C10)	5.00	180. 00
47	(C9)-(C14)-(C13)-(S11)	9.74	180.00
48	(C13)-(S11)-(C10)-(N12)	3.95	180.00
49	(S11)-(C10)-(N12)-(C14)	19.48	180.00
50	(C13)-(S11)-(C10)-(C19)	3.95	180.00
51	(S11)-(C10)-(C19)-(C17)	2.50	180.00
52	(S11)-(C10)-(C19)-(C20)	2.50	180.00
53	(C10)-(S11)-(C13)-(C14)	3.95	180.00
54	(C14)-(N12)-(C10)-(C19)	19.48	180.00
55	(N12)-(C10)-(C19)-(C17)	2.50	180.00
56	(N12)-(C10)-(C19)-(C20)	2.50	180.00
57	(C10)-(N12)-(C14)-(C13)	5.00	180.00
58	(C10)-(C19)-(C17)-(C15)	9.74	180.00
59	(C10)-(C19)-(C17)-(H32)	9.74	180.00
60	(C10)-(C19)-(C20)-(C18)	2.50	180.00
61	(C10)-(C19)-(C20)-(H34)	2.50	180.00
62	(S11)-(C13)-(C14)-(N12)	9.74	180.00
63	(C18)-(C16)-(C15)-(C17)	9.74	180.00
64	(C16)-(C15)-(C17)-(C19)	2.50	180.00
65	(C16)-(C15)-(C17)-(H32)	2.50	180.00
66	(C36)-(C15)-(C16)-(C18)	9.74	180.00
67	(C15)-(C16)-(C18)-(C20)	2.50	180.00
68	(C15)-(C16)-(C8)-(H33)	2.50	180.00
69	(C36)-(C15)-(C17)-(C19)	2.50	180.00
70	(C15)-(C17)-(C19)-(C20)	9.74	180.00
71	(H32)-(C17)-(C15)-(C36)	2.50	180.00
72	(C16)-(C18)-(C20)-(C19)	9.74	180.00
73	(C16)-(C18)-(C20)-(H34)	9.74	180.00
74	(H32)-(C17)-(C19)-(C20)	9.74	180.00
75	(C17)-(C19)-(C20)-(C18)	2.50	180.00
76	(C17)-(C19)-(C20)-(H34)	2.50	180.00
77	(H33)-(C18)-(C20)-(C19)	9.74	180.00
78	(H34)-(C20)-(C18)-(H33)	9.743	180.00

Table 5: Calculated energy and difference after each cycle of febuxostate.

Cycle	Energy	difference
1	1.389776	0
2	-62.615657537	-64.0054
3	-15.155315548	47.4603
4	-87.248439673	-72.0931
5	-94.327447752	-7.07901
6	-101.141148607	-6.8137
7	-104.675100265	-3.53395
8	-107.544118016	-2.86902
9	-103.811981893	3.73214
10	-105.453407657	-1.64143
11	-107.631929378	-2.17852
12	-109.072573823	-1.44064
13	-110.848326308	-1.77575
14	-117.432767105	-6.58444
15	-123.604076576	-6.17131
16	-124.001990148	-0.397914
17	-106.482997834	17.519
18	-112.495419579	-6.01242
19	-113.094909557	-0.59949
20	-114.350843254	-1.25593
21	-116.945533212	-2.59469
22	-115.051786057	1.89375
23	-93.748537561	21.3032
24	-110.744033088	-16.9955
25	-113.921474173	-3.17744
26	-113.004825625	0.916649
27	-105.036954750	7.96787
28	-112.676954329	-7.64
29	-114.968454573	-2.2915
30	-113.495936488	1.47252
31	-111.966016592	1.52992
32	-113.631769311	-1.66575
33	-114.486262893	-0.854494
34	-116.041903154	-1.55564
35	-120.335451873	-4.29355
36	-124.484040858	-4.14859
37	-124.601231979	-0.117191
38	-119.593432336	5.0078
39	-112.808400304	6.78503
40	-116.302507786	-3.49411
41	-117.750211161	-1.4477
42	-121.513605489	-3.76339
43	-125.831931320	-4.31833
44	-125.391772810	0.440159
45	-119.627602209	5.76417
46	-82.778390011	36.8492
47	-109.434897420	-26.6565
48	-112.193391450	-2.75849
49	-105.031710998	7.16168
50	-109.517902070	-4.48619
51	-101.673535989	7.84437
52	-108.701377407	-7.02784
53	-109.957325606	-1.25595
54	-109.292922445	0.664403
55	-107.991851990	1.30107
56	-111.113203362	-3.12135
57	-113.022859335	-1.90966
58	-119.665964234	-6.6431
59	-124.512152090	-4.84619
60	-124.910541899	-0.39839
61	-121.844292541	3.06625
62	-93.130077786	28.7142
63	-108.206451698	-15.0764
64	-110.307320509	-2.10087
65	-108.635647236	1.67167
66	-105.012599714	3.62305
67	-110.018140383	-5.00554

68	-112.406751993	-2.38861
69	-105.626254538	6.7805
70	-110.690230877	-5.06398
71	-111.414150637	-0.72392
72	-112.733984839	-1.31983
73	-117.808616248	-5.07463
74	-112.369692183	5.43892
75	-99.158016593	13.2117
76	-110.926656007	-11.7686
77	-114.402256366	-3.4756
78	-113.386362908	1.01589
79	-106.216575902	7.16979
80	-105.933712636	0.282863
81	-109.206350860	-3.27264
82	-110.677284578	-1.47093
83	-112.588425238	-1.91114
84	-116.689313293	-4.10089
85	-110.991530190	5.69778
86	-109.176067460	1.81546
87	-113.070115867	-3.89405
88	-114.903368458	-1.83325
89	-118.934046450	-4.03068
90	-114.018292350	4.91575
91	-110.090193771	3.9281
92	-113.701546142	-3.61135
93	-115.082909073	-1.38136
94	-117.810706439	-2.7278
95	-122.573167004	-4.76246
96	-124.945038401	-2.37187
97	-126.201011017	-1.25597
98	-126.775608772	-0.574598
99	-127.138034669	-0.362426
100	-127.411373096	-0.273338
101	-127.578788188	-0.167415
102	-127.834941685	-0.256153
103	-128.195098146	-0.360156
104	-128.365887970	-0.17079
105	-128.430689109	-0.0648011
106	-128.441671585	-0.0109825
107	-128.442352106	-0.000680521
108	-128.442429574	-7.74679e-005
109	-128.442448689	-1.91145e-005
110	-128.442455115	-6.42594e-006
111	-128.442457298	-2.18333e-006
112	-128.442458228	-9.29631e-007
113	-128.442458645	-4.17682e-007
114	-128.442458846	-2.00146e-007
115	-128.442458964	-1.18534e-007
116	-128.442459048	-8.41991e-008
117	-128.442459114	-6.55491e-008
118	-128.442459174	-5.98127e-008
119	-128.442459229	-5.53387e-008
120	-128.442459280	-5.08469e-008
121	-128.442459326	-4.62676e-008
122	-128.442459371	-4.46283e-008
123	-128.442459413	-4.18314e-008
124	-128.442459451	-3.83261e-008
125	-128.442459488	-3.74123e-008
126	-128.442459523	-3.48178e-008
127	-128.442459556	-3.27332e-008
128	-128.442459587	-3.07745e-008
129	-128.442459616	-2.89252e-008
130	-128.442459643	-2.7193e-008
131	-128.442459668	-2.51546e-008
132	-128.442459692	-2.41838e-008
133	-128.442459714	-2.22929e-008
134	-128.442459736	-2.1372e-008
135	-128.442459756	-1.99873e-008
136	-128.442459775	-1.8797e-008
137	-128.442459792	-1.76693e-008
138	-128.442459809	-1.66062e-008
139	-128.442459824	-1.56122e-008
140	-128.442459839	-1.46787e-008
141	-128.442459853	-1.38002e-008
142	-128.442459866	-1.29706e-008
143	-128.442459878	-1.21953e-008
144	-128.442459890	-1.14602e-008
145	-128.442459900	-1.07776e-008
146	-128.442459910	-1.01298e-008
147	-128.442459920	-9.52343e-009
148	-128.442459929	-8.94738e-009
149	-128.442459937	-8.41612e-009
150	-128.442459945	-7.91306e-009
151	-128.442459953	-7.43785e-009
152	-128.442459960	-6.98935e-009
153	-128.442459966	-6.57246e-009
154	-128.442459972	-6.17581e-009
155	-128.442459978	-5.81224e-009
156	-128.442459984	-5.45776e-009
157	-128.442459989	-5.13478e-009
158	-128.442459994	-4.82248e-009
159	-128.442459998	-4.53781e-009
160	-128.442460002	-4.26417e-009
161	-128.442460006	-4.00462e-009
162	-128.442460010	-3.76895e-009
163	-128.442460014	-3.54453e-009
164	-128.442460017	-3.33137e-009
165	-128.442460020	-3.12536e-009
166	-128.442460023	-2.94415e-009
167	-128.442460026	-2.76577e-009
168	-128.442460029	-2.59934e-009
169	-128.442460031	-2.44597e-009
170	-128.442460033	-2.29409e-009
171	-128.442460035	-2.16119e-009
172	-128.442460037	-2.02942e-009
173	-128.442460039	-1.91369e-009
174	-128.442460041	-1.79159e-009
175	-128.442460043	-1.687e-009
176	-128.442460044	-1.58434e-009
177	-128.442460046	-1.48918e-009
178	-128.442460047	-1.39948e-009
179	-128.442460049	-1.31786e-009
180	-128.442460050	-1.2393e-009
181	-128.442460051	-1.16631e-009
182	-128.442460052	-1.09287e-009
183	-128.442460053	-1.03068e-009
184	-128.442460054	-9.66111e-010
185	-128.442460055	-9.07676e-010
186	-128.442460056	-8.54925e-010
187	-128.442460057	-8.00583e-010
188	-128.442460057	-7.55335e-010
189	-128.442460058	-7.12475e-010
190	-128.442460059	-6.66205e-010
191	-128.442460059	-6.25619e-010
192	-128.442460060	-5.91285e-010
193	-128.442460061	-5.50244e-010
194	-128.442460061	-5.23869e-010
195	-128.442460062	-4.90445e-010
196	-128.442460062	-4.58613e-010
197	-128.442460063	-4.33602e-010
198	-128.442460063	-4.0518e-010
199	-128.442460063	-3.84489e-010
200	-128.442460064	-3.59023e-010

CONCLUSION

By using Argus Lab software, the present work clearly shows that the best conformation of Febuxostat molecule is found to be at -80598.93. At this point, drug is more active as an antigout agent.

In this work it is shown that conformational analysis with minimum potential energy is crucial when establishing SAR/QSAR models using theoretically calculated descriptors, since it can be dependent on the molecular structure. Finally all geometric variables were completely optimized for each compound and the lowest energy conformations were used in molecular modeling studies.

REFERENCES

1. Lawrence RC, Helmick CG and Arnett FC. Estimates of the prevalence of arthritis and selected musculoskeletal disorders in the United States. *Arthritis Rheum.,* 1998; 41: 778-799.
2. Yu KH and Luo SF. Younger age of onset of gout in Taiwan. *Rheumatology,* 2003; 42: 166-170.
3. Chang HY, Pan WH, Yeh WT and Tsai KS. Hyperuricemia and gout in Taiwan: results from the Nutritional and Health Survey in Taiwan (1993-96). *J. Rheumatol.,* 2001; 28: 1640-1646.
4. Tom GR and Kelsey MJ. The modern management of gout. *Rheumatology,* 2010; 49: 5–14.
5. Choi HK. Pathogenesis of gout. *Ann. Intern. Med.,* 2005; 143: 499-516.
6. Zhang W. EULAR evidence based recommendations for gout. Part II: Management. Report of a task force of the Standing Committee for International Clinical Studies Including Therapeutics (ESCISIT). *Ann. Rheum. Dis.,* 2006; 65: 1312-1324.
7. Eliseo P. Febuxostat: *Nature Rev.-Drug Disc.,* 2009: 8: 191-192.
8. Wortmann R and Kelly WN. Gout and hyperuriciemia. In: Firestein GS, Budd RC, Harris EO, et al. editors. *Kelley's Textbook of Rheumatology*. 8th ed. Philadelphia, PA: Saunders Elsevier; 2008: pp 1481-1586.
9. Arellano F and Sacristan JA. Allopurinol hypersensitivity syndrome: a review. *Ann. Pharmacother.,* 1993; 27: 337-343.
10. Lada BL, Michael HP and David SG. Advances in the management of gout. Critical appraisal of febuxostat in the control of hyperuricemia. *Int. J. Nephrol. Renovasc. Dis.,* 2010; 3: 31-10.
11. Okamoto K. An extremely potent inhibitor of xanthine oxidoreductase. Crystal structure of the enzyme inhibitor complex and mechanism of inhibition. *J. Biol. Chem.,* 2003; 278: 1848-1855.
12. Khosravan R, Grabowski BA, Wu JT, Joseph-Ridge N and Vernillet L. Pharmacokinetics, pharmacodynamics and safety of febuxostat, a non-purine selective inhibitor of xanthine oxidase, in a dose escalation study in healthy subjects. *Clin. Pharmacokinet.,* 2006; 45: 821-841.
13. Schumacher HR Jr. Febuxostat: a non-purine, selective inhibitor of xanthine oxidase for the management of hyperuricaemia in patients with gout. *Expert Opin. Investig. Drugs,* 2005; 14: 893- 903.
14. Angelo L Gaffo and Kenneth GS. Febuxostat: the evidence for its use in the treatment of hyperuricemia and gout. Dove Press, 2009: 4: pp 25-36.
15. Bhakat S. Conformational analysis (geometry optimization) of chemotherapic agent Cytarabine by Argus Lab Software. *Int. J. Phsic. Sci.,* 2011; 3: 1221-1227.
16. Khalida Bano. Conformational analysis of flavanoid derivative as histamine H1 receptor antagonist. *Pak. J. Biochem. Mol. Biol.,* 2010; 43: 109-113.
17. Loew GH, Villar HO and Alkorta I. Strategies for indirect computer-aided drug design. *Pharmaceut. Res.,* 1993; 10: 475-486.
18. Csizmadia IG and Enriz RD. Peptide and protein folding. *J. Mol. Struct.-Theochem.,* 2001; 543: 319-361.